



Research article

Synergistic effects of *Momordica charantia*, *Nigella sativa*, and *Anethum graveolens* on metabolic syndrome targets: *In vitro* enzyme inhibition and in silico analyses

Rajashekar S. Chavan^a, Nayeem A. Khatib^{a,*}, M.G Hariprasad^b, Vishal S. Patil^a, Moqbel Ali Moqbel Redhwan^b

^a Department of Pharmacology, KLE College of Pharmacy, Belagavi, KLE Academy of Higher Education and Research, Belagavi 590010, Karnataka, India

^b Department of Pharmacology, KLE College of Pharmacy, Bengaluru, Karnataka, India

ARTICLE INFO

Keywords:

Momordica charantia

Anethum graveolens

Pancreatic lipase inhibition

Molecular docking

Dynamics simulation

ABSTRACT

Momordica charantia, *Nigella sativa*, and *Anethum graveolens* are established medicinal plants possessing noted anti-diabetic and anti-obesity properties. However, the molecular mechanisms underscoring their inhibitory effects on pancreatic lipase, α -glucosidase, and HMG-CoA reductase remain unexplored. This study aimed to elucidate the efficacy of various NS, MC, and AG blends in modulating the enzymatic activity of pancreatic lipase, HMG-CoA reductase, and α -glucosidase, utilizing an integrative approach combining *in vitro* assessments and molecular modeling techniques. A factorial design matrix generated eight distinct concentration combinations of NS, MC, and AG, subsequently subjected to *in vitro* enzyme inhibition assays. Molecular docking analyses using AutoDock Vina, molecular dynamics simulations, MMPBSA calculations, and principal component analysis, were executed with Gromacs to discern the interaction dynamics between the compounds and target enzymes. A formulation comprising NS:MC:AG at a 215:50:35 $\mu\text{g}/\text{mL}$ ratio yielded significant inhibition of pancreatic lipase (IC_{50} : $74.26 \pm 4.27 \mu\text{g}/\text{mL}$). Moreover, a concentration combination of 215:80:35 $\mu\text{g}/\text{mL}$ effectively inhibited both α -glucosidase (IC_{50} : $66.09 \pm 3.98 \mu\text{g}/\text{mL}$) and HMGCR (IC_{50} : $129.03 \mu\text{g}/\text{mL}$). Notably, MC-derived compounds exhibited superior binding affinity towards all three enzymes, compared to their reference molecules, with diosgenin, Momordicoside I, and diosgenin displaying binding affinities of -11.0 , -8.8 , and -7.9 kcal/mol with active site residues of pancreatic lipase, α -glucosidase, and HMGCR, respectively. Further, 100 ns molecular dynamics simulations revealed the formation and stabilization of non-bonded interactions between the compounds and the enzymes' active site residues. Through a synergistic application of *in vitro* and molecular modeling methodologies, this study substantiated the potent inhibitory activity of the NS:MC:AG blend (at a ratio of 215:80:35 $\mu\text{g}/\text{mL}$) and specific MC compounds against pancreatic lipase, α -glucosidase, and HMGCR. These findings provide invaluable insights into the molecular underpinnings of these medicinal plants' anti-diabetic and anti-obesity effects and may guide future therapeutic development.

* Corresponding author. Head of Department of Pharmacology, KLE College of Pharmacy, Belagavi, KLE Academy of Higher Education and Research, Belagavi 590010, Karnataka, India.

E-mail address: khatibnayeem@hotmail.com (N.A. Khatib).

<https://doi.org/10.1016/j.heliyon.2024.e24907>

Received 14 October 2023; Received in revised form 16 January 2024; Accepted 17 January 2024

Available online 18 January 2024

2405-8440/© 2024 The Authors. Published by Elsevier Ltd. This is an open access article under the CC BY-NC-ND license (<http://creativecommons.org/licenses/by-nc-nd/4.0/>).

1. Introduction

Metabolic Syndrome (MetS) is a confluence of medical conditions including hypertension, high blood sugar, insulin resistance, obesity, and abnormal lipid profiles, cumulatively elevating the risk of type 2 diabetes mellitus (T2DM), cardiovascular disease (CVD), and stroke [1,2]. With the global surge in T2DM and CVD, MetS has garnered attention as a significant health concern. Unlike infectious diseases and acute disorders, MetS is insidious, often taking years to manifest with variable presentations across individuals [2].

The pathogenesis of MetS is intricate and not fully elucidated. It is debatable whether the myriad symptoms of MetS are manifestations of a singular pathological process or indicative of distinct diseases. Empirical evidence highlights increased caloric intake as a primary precipitant for MetS, engendering particularly visceral adiposity [3]. Among the various hypothesized pathways implicated in MetS, insulin resistance, neurohormonal activation, and chronic inflammation are pivotal in its onset, progression, and transition to CVD [4].

Postprandial hyperglycemia, characterized by spikes in blood glucose levels following meals, is influenced by diverse factors like composition and the balance of insulin and glucagon production. Beyond its association with obesity, hypertension, and endothelial dysfunction, uncontrolled hyperglycemia is implicated in the onset of diabetes mellitus and its myriad complications, including organ failure [5]. This study focuses on three enzymes, namely pancreatic lipase (PNLIP), α -glucosidase (GAA), and HMG-CoA reductase (HMGCR), identified as prospective therapeutic targets for MetS. PNLIP, secreted by the pancreas into the duodenum, plays a crucial role in the hydrolysis and digestion of fats, cholesterol esters, and fat-soluble vitamins, making it an apt target for obesity treatment. GAA, on the other hand, facilitates the breakdown of polysaccharides into monosaccharides, thereby contributing to postprandial hyperglycemia [6,7]. Inhibiting GAA at the small intestine's brush border effectively modulates glucose absorption, a strategy extensively employed in DM treatment [8–10]. Similarly, HMGCR catalyzes the conversion of HMG-CoA to mevalonic acid, a requisite step in cholesterol biosynthesis. Antagonists of HMGCR are vital in managing hypercholesterolemia and CVD, with statins being the drug of choice. However, recent clinical trials, notably the double-blind JUPITER and PROSPER studies, have reported an increased incidence of T2DM among statin users [11–13].

Numerous bioactive compounds found in foods, vegetables, and herbs have been reported and validated for their metabolic functions and potential in treating, managing, and preventing various diseases, including inflammation, oxidative stress, CVD, dyslipidemia, and DM [14,15]. In this research, we have selected *Nigella sativa* (seed), *Momordica charantia* (fruit), and *Anethum graveolens* L (fruit) for their established use in MetS management. We prepared a polyherbal formulation using a Three-factor, 2-level factorial design, with varying concentrations of the selected herbs as followed by the previous literature [16,17]. This paper elucidates the mode of action of these formulations in inhibiting PNLIP, GAA, and HMGCR, as assessed by *in vitro* assays and *in silico* molecular docking and dynamics studies.

2. Methods

2.1. *In vitro* pharmacology

2.1.1. Collection, authentication, and extract preparation

Seeds of *Nigella sativa* L. and fruits of *Anethum graveolens* and *Momordica charantia* L. were collected in September–October 2020 from the Belagavi region, Karnataka. These were identified and authenticated at Shri B.M.K Ayurveda Pharmacy, Belagavi, receiving authentication numbers CRF/Auth/2020/03, CRF/Auth/2020/04, and CRF/Auth/2020/05, respectively. The plant materials were washed, dried, and ground into coarse powder. Cold maceration with 75 % v/v ethanol was performed on the powder for seven days to extract thermolabile constituents. The filtrate obtained was then concentrated using rotary evaporation at 40 °C under reduced pressure, followed by a three-day lyophilization process. The final extract yields for *Anethum graveolens*, *Momordica charantia*, and *Nigella sativa* were 1.25 %, 1.75 %, and 2.13 %, respectively.

2.1.2. Preparation and optimization of herbal formulation

A three-factor, two-level factorial design was utilized for the preparation and optimization of herbal formulations. The factors, represented by three herbal drugs, were evaluated at two levels: low (0) and high (+1). Specifically, the factors were the hydroalcoholic extracts of *Nigella sativa* (HAENS), *Momordica charantia* (HAEMC), and *Anethum graveolens* (HAEAG). For HAENS (Factor 1), the low and high levels were set at 110 and 215, respectively. For HAEMC (Factor 2), the levels were 50 (low) and 80 (high), and for HAEAG (Factor 3), the levels were set at 25 (low) and 35 (high). Employing these defined levels for each factor, eight different concentration combinations were formulated. These combinations represented eight distinct ratios of NS:MC:AG, namely: 110:50:25, 110:50:35, 110:80:25, 110:80:35, 215:50:25, 215:50:35, 215:80:25, and 215:80:35. These experimental trials were meticulously designed using Systat software (version 13.2, USA) to explore the various concentration combinations of the herbal drugs in the formulation [18,19]. Each combination was then assessed and analyzed to establish optimal conditions for the herbal formulation.

2.2. Estimation of total phenolic, flavonoid, and tannin contents

2.2.1. Total phenolic content (TPC) estimation

The TPC of the extracts was quantified using the Folin-Ciocalteu (FC) reagent, adhering to the methodology outlined by Singleton et al. (1999) [20]. Initially, 3 mL of diluted extract was combined with 0.5 mL of FC reagent. After a 10-min incubation at room

temperature, 2 mL of 7 % Na₂CO₃ solution was added to the mixture. Following a 1-min boiling period, the absorbance of the resulting color was measured at 750 nm with a Shimadzu UV-1800 spectrophotometer (Kyoto, Japan). The TPC results were reported in micrograms of Gallic Acid Equivalent ($\mu\text{g GAE}$) per milligram of extract.

2.2.2. Flavonoid content estimation

For flavonoid content estimation, the procedure established by Delcour and Varebeke (1985) was followed [21]. 1 mL of diluted extract was mixed with 5 mL of chromogen reagent. After incubating for 10 min, absorbance was measured at 640 nm. The flavonoid content was expressed in micrograms of Quercetin Equivalent ($\mu\text{g QE}$) per milligram of extract.

2.2.3. Tannin content estimation

Total tannin content was determined based on the protocol described by Makkar et al. (2003) [22]. An aliquot (0.05 mL) of each sample was diluted to 0.5 mL with distilled water, followed by the addition of 0.25 mL of 1 N Folin-Ciocalteu reagent. This mixture was then combined with 1.25 mL of 20 % sodium carbonate solution, incubated for 40 min, and vortexed. Absorbance was recorded at 725 nm, with tannin content results being expressed as micrograms of Tannic Acid Equivalent ($\mu\text{g TAE}$) per milligram of extract.

2.3. Antioxidant activity measurement

2.3.1. DPPH free radical scavenging assay

The antioxidant activities of the samples were assessed through their ability to scavenge DPPH (2,2-diphenyl-1-picrylhydrazyl) free radicals, following the method proposed by Blois (1958) [23]. Different concentrations of samples, spanning from 100 to 300 $\mu\text{g/mL}$, were prepared. For each assay, the respective sample concentration (1 mL) was mixed with 2 mL of a 100 μM DPPH solution. The total volume of the reaction mixture was adjusted to 3 mL with methanol. To allow the reaction to proceed, the mixture was incubated in the dark at room temperature for 45 min. Following incubation, the absorbance of each reaction mixture was measured at 517 nm against a blank (methanol without sample or standard antioxidant) via a UV-1800 spectrophotometer (Kyoto, Japan). The DPPH radical scavenging activity of each sample was then quantified by calculating the half-maximal inhibitory concentration (IC₅₀) values and expressed relative to the standard antioxidant, butylated hydroxytoluene (BHT).

2.4. In-vitro enzyme inhibition assay

2.4.1. Pancreatic lipase inhibitory activity

Following the methodologies of Bustanji et al. [24] and Zheng et al. [25], with slight modifications, the inhibitory activity of sample combinations against pancreatic lipase was assessed. Stock solutions of samples/extracts (10 mg/mL) and pancreatic lipase enzyme (1 mg/mL) were prepared, the latter freshly prepared before use. The Working solution of *p*-nitrophenyl butyrate (PNPB) was obtained by dissolving 20.9 mg in 2 mL of acetonitrile, using 100 μL for the assay. For the reaction, samples were mixed with enzyme solution, adjusted to 1 mL with Tris-HCl (pH 7.4), and incubated at 25 °C for 15 min. Post incubation, 100 μL of PNPB was added, followed by an additional 30-min incubation at 37 °C. The lipase activity was evaluated by monitoring the conversion of PNPB to *p*-nitrophenol at 405 nm, with inhibition percentages calculated relative to the blank, and results expressed as IC₅₀ values.

2.4.2. α -glucosidase inhibitory activity assay

The evaluation of α -glucosidase inhibitory activities in various samples was conducted as described by Khanal and Patil [8,26]. Initially, the α -glucosidase enzyme was dissolved in a 50 mM phosphate buffer solution, with a pH of 6.9. This enzyme solution was then independently pre-treated with different concentrations of the test samples, ranging from 0 to 125 $\mu\text{g/mL}$, and incubated for 10 min at a temperature of 37 °C. Following this pre-treatment, the reaction was initiated by adding 50 μL of 5 mM *p*-Nitrophenyl- α -D-glucopyranoside (*p*-NPG) in phosphate buffer to each sample. The enzymatic reaction was then allowed to proceed for 30 min at 37 °C. To terminate the reaction, 1 M sodium carbonate (Na₂CO₃) was added. The absorbance of the resulting solution was measured at 405 nm. The results were expressed as IC₅₀ values, which indicate the concentration of the test sample required to inhibit 50 % of the enzyme activity, and were compared with acarbose, used as a positive control.

2.4.3. HMG-CoA reductase inhibitory activity assay

The assessment of the inhibitory effect of various samples on HMG-CoA reductase was adapted from an established method by Salvamani et al., [27]. Different concentrations of each sample, ranging from 0 to 125 μg , were combined with a reaction mixture. This mixture comprised of 400 μM NADPH, 400 μM HMG-CoA as the substrate, and a potassium phosphate buffer (100 mM, pH 7.4). Subsequently, 5 μL of HMG-CoA reductase was added. The mixture was then incubated at a temperature of 37 °C. After an incubation period of 10 min, the absorbance was measured at a wavelength of 340 nm to determine the activity. For comparative purposes, Simvastatin was employed as a standard reference (positive control), while distilled water or a sample-free solution served as the negative control. The percentage of HMG-CoA reductase inhibition was determined using the formula (Gholamhoseinian et al., 2010). Inhibition (%) = (Absorbance of control – Absorbance test/Absorbance of control) \times 100,100 and the results were expressed in IC₅₀ values by using a linear regression curve.

2.5. *In silico* pharmacology

2.5.1. Molecular docking

2.5.1.1. Ligand preparation. 3D conformers of phytochemicals and standard molecules were retrieved from the PubChem database in.sdf format. These were then converted into.pdb format using Discovery Studio 2019. Each ligand underwent energy minimization using the MMFF94 force field and the conjugate gradient optimization algorithm, subsequently being converted into.pdbqt format.

2.5.1.2. Macromolecule preparation. 3D structures of PNLIP (PDB ID: 1LPB) [28], α -glucosidase (PDB ID: 5NN8) [29], and HMGCR (PDB ID: 1HW9) [30] were obtained from the RCSB Protein Data Bank. Water molecules and other heteroatoms were removed using Discovery Studio 2019, with the cleaned structures saved in.pdb format.

2.5.1.3. Ligand-protein docking. The prepared ligands were docked into their respective targets using the POAP pipeline of AutoDock Vina [31]. For PNLIP, the grid center was set at $x = 9.188$, $y = 24.612$, $z = 50.508$, with a grid size of 26 (x,y,z). For α -glucosidase, the grid center and size were $x = -15.85$, $y = -32.64$, $z = 95.42$ and $x = 30.29$, $y = 31.72$, $z = 34.88$, respectively. For HMGCR, the center was $x = 1.45$, $y = -6.66$, $z = -9.43$ with a grid size of $x = 29.0$, $y = 34.74$, $z = 32.45$. Docking was executed with system exhaustiveness set at 20, generating nine conformations. The ligand conformation exhibiting the lowest binding energy and RMSD was selected for subsequent visualization in Discovery Studio 2019.

2.5.2. Molecular dynamics simulation

Molecular dynamics simulations were conducted using Gromacs version 2022.1 [32]. The Amber antechamber ff99SBildn force-field was utilized to generate the topologies of both proteins and ligands through the xleap module. The proteins were immersed in a dodecahedron simulation box with a three-point water model, ensuring a minimum distance of 10.0 Å from the box edges. Charge neutrality in the system was attained by the addition of sodium and chloride ions as required. The process commenced with an energy minimization phase, employing the steepest descent integrator and a Verlet cutoff scheme. This phase was carried out for up to 50,000 steps, or until the point where the proteins reached a state of minimum energy conformation. Following this, the system was equilibrated in two phases: the canonical (NVT) ensemble and the isobaric-isothermal ensemble, with each phase lasting for 100 ps. Temperature control during the simulations was maintained at 300 K using the V-rescale thermostat, and a constant pressure of 1 bar was upheld by the C-rescale algorithm. Finally, a comprehensive 100 ns molecular dynamics simulation was conducted for each protein-ligand complex. During these simulations, the coordinates and energies were captured every 20 ps. The resulting trajectories and their corresponding outcomes were analyzed using the inherent utilities of Gromacs, supplemented by various external analytical tools as necessary.

2.5.3. MMPBSA calculation

The gmx MMPBSA module [33] was utilized for MMPBSA analysis, focusing on different energy-contributing factors such as molecular mechanics energies in the form of van Der Waals and electrostatic interactions, the complete energy of solvation, and the aggregate relative energy of binding. The analysis involved a total of 5000 frames, sampled at intervals of 500 frames [34].

2.5.4. Principal component analysis (PCA)

PCA, a robust statistical technique, was employed to identify significant collective motions in biomolecular simulations. This approach is instrumental in analyzing how domain movements contribute to protein folding and unfolding processes. By transforming the protein conformation coordinates orthogonally, principal components (PCs) are generated [34]. In this study, PCA was executed to investigate the predominant modes governing the dynamics of biomolecules. This involved generating a covariance matrix and diagonalizing said matrix through the use of Gromacs utilities "g_covar" and "g_anaeig", facilitating the investigation of the biomolecular dynamics at play.

3. Results

3.1. Total phenol, flavonoid, and tannin contents estimation

In a comparative study of different sample batches, it was found that Sample 08, optimized at a ratio of 215:80:35 (NS:MC:AG), exhibited the highest concentrations of bioactive compounds among the tested samples. Specifically, Sample 08 revealed the highest content of total polyphenols (286.69 ± 5.58 µg/mg GAE), flavonoids (95.05 ± 4.19 µg/mg QE), and tannins (17.31 ± 1.42 µg/mg TAE). These results underscore the superior polyphenolic profile of Sample 08, highlighting its potential significance in applications where these bioactives are of paramount importance.

4. DPPH antioxidant potential of samples

In the assessment of the DPPH antioxidant properties among different sample batches, Butylated hydroxytoluene (BHT) was employed as a standard, demonstrating an IC₅₀ value of 14.06 ± 1.64 µg/mL. Comparatively, Sample 06, formulated at a ratio of

215:50:35 (NS:MC:AG), displayed an IC₅₀ value of 82.43 ± 3.67 $\mu\text{g/mL}$, while Sample 08, with a 215:80:35 ratio, recorded 108.86 ± 4.82 $\mu\text{g/mL}$. Sample 07, optimized at 215:80:25, had an IC₅₀ of 120.48 ± 5.65 $\mu\text{g/mL}$. Notably, both Sample 06 and Sample 08 showcased enhanced radical scavenging activity relative to the BHT standard, indicating their promising antioxidant potential.

4.1. Pancreatic lipase inhibitory activity

There was concentration-dependent inhibition of pancreatic lipase by formulations (Table 1). The NS:MC:AG at ratio 215:50:35 (formulation No. 6) exhibited a notable inhibitory effect on pancreatic lipase with IC₅₀ of 74.26 ± 4.27 $\mu\text{g/mL}$, whereas, orlistat IC₅₀ was found to be 57.01 ± 2.97 $\mu\text{g/mL}$ (linearity $y = 0.745x + 9.143$, $R^2 = 0.956$); suggesting is approximately 0.23 times less effective than orlistat. Likewise, NS:MC:AG at ratio 215:80:25 (formulation No. 7) and ratio 215:80:35 (formulation No. 8) were second and third lead formulations for pancreatic lipase inhibition with IC₅₀ of 82.34 ± 4.14 and 91.65 ± 3.81 , respectively.

4.2. α -glucosidase inhibitory activity

The study demonstrated a variable inhibition of α -glucosidase by different formulations (Table 1). The NS:MC:AG at ratio 215:80:35 (formulation No. 8) exhibited a significant inhibitory effect on α -glucosidase, achieving IC₅₀ of 66.09 ± 3.98 $\mu\text{g/mL}$, whereas, acarbose IC₅₀ was found to be 47.66 ± 1.80 $\mu\text{g/mL}$ (linearity $y = 0.9242x + 4.77$, $R^2 = 0.992$); suggesting it was approximately 27 % less effective than acarbose. Likewise, NS:MC:AG at ratio 215:80:25 (formulation No. 7) and ratio 215:50:35 (formulation No. 6) were second and third lead formulations for pancreatic lipase inhibition with IC₅₀ of 70.44 ± 4.18 and 89.74 ± 4.37 , respectively.

4.3. HMG-CoA reductase inhibitory activity

There is no concentration-dependent inhibition of HMG-CoA reductase by formulations (Table 1). However, only NS:MC:AG at ratio 215:80:35 (formulation No. 8) showed moderate inhibitory activity against HMG-CoA reductase with IC₅₀ of 129.03 $\mu\text{g/mL}$, whereas, simvastatin IC₅₀ was found to be 52.62 $\mu\text{g/mL}$ (linearity $y = 0.9896x - 2.0809$, $R^2 = 0.9895$); The efficacy of the compound was determined to be approximately 0.59 times lower than that of simvastatin. All other formulation IC₅₀ range was found to be within 165 to 140 $\mu\text{g/mL}$.

4.4. Molecular docking of compounds with PNLIP, GAA, and HMGCR

Diosgenin demonstrates a superior binding affinity to PNLIP, evidenced by a binding energy of -11.0 kcal/mol, featuring 18 hydrophobic bonds and interactions with residues including Ile209, Pro180 (4), Tyr114 (4), Phe77 (2), Phe215 (4), Ile78, His263, and Ala260. This is more effective compared to acarbose, which shows a binding energy of -7.1 kcal/mol, forming 2 hydrogen bonds with Arg256 and His151, and 9 hydrophobic bonds with residues Ile209, Ile78, Trp252 (2), Pro180, Phe215, Trp114, Ser152, and Gly76. Furthermore, diosgenin also exhibits a higher affinity for HMGCR, with a binding energy of -7.9 kcal/mol. This includes 1 hydrogen bond with Val772 and 4 hydrophobic bonds with Leu858, Ala754 (3). In contrast, Simvastatin has a lower binding energy of -5.2 kcal/mol, forming 2 hydrogen bonds with Ser745 and Lys735, and 4 hydrophobic bonds with Ala754 (4). Similarly, Momordicoside-I shows greater binding affinity towards GAA, with a binding energy of -8.8 kcal/mol. It forms 3 hydrogen bonds with Asp356, Met363, Arg594, and 6 hydrophobic bonds with Leu283, Gly549, Ala555, Trp481 (2), and Met519. This is in comparison to acarbose, which has a binding energy of -6.1 kcal/mol, establishing 2 hydrogen bonds with Ala555, Asp404, and 3 hydrophobic bonds with Arg608, His584, and His717 (Fig. 1a-f and Table 2).

Table 1

In-vitro enzyme inhibition Assay: pancreatic lipase, α -Glucosidase, and HMG CoA.

S. No	Optimization Batch (NS:MC:AG)	Pancreatic lipase IC ₅₀ in $\mu\text{g/mL}$	α -Glucosidase IC ₅₀ in $\mu\text{g/mL}$	HMGCR IC ₅₀ in $\mu\text{g/mL}$
Orlistat*	–	57.01 ± 2.97	–	–
Acarbose*	–	–	47.66 ± 1.80	–
Simvastatin*	–	–	–	52.62
01	110:50:25	133.00 ± 4.78	109.03 ± 4.72	165.02
02	110:50:35	148.02 ± 5.15	117.74 ± 3.34	162.56
03	110:80:25	168.36 ± 3.96	153.23 ± 5.68	158.26
04	110:80:35	186.28 ± 5.00	123.78 ± 6.09	155.02
05	215:50:25	142.91 ± 5.19	110.44 ± 5.59	157.05
06	215:50:35	74.26 ± 4.27	89.74 ± 4.37	154.37
07	215:80:25	82.34 ± 4.14	70.44 ± 4.18	140.36
08	215:80:35	91.65 ± 3.81	66.09 ± 3.98	129.03

In silico studies.

Table 2

Binding affinity, hydrogen, and non-hydrogen bonds count, and residue of each target for top scoring respective ligand.

Targets	Ligand	Binding affinity (kcal/mol)	No. of HBR	No. of NHBR	HBR	NHBR
PNLIP (PDB: 1LPB)	Diosgenin	-11.0	0	18	Nil	Ile209, Pro180 (4), Tyr114 (4), Phe77 (2), Phe215 (4), Ile78, His263, Ala260
	Orlistat ^a	-7.1	2	9	Arg256, His151	Ile209, Ile78, Trp252 (2), Pro180, Phe215, Trp114, Ser152, Gly76
α -glucosidase (PDB: 5NN8)	Momordicoside-I	-8.8	3	6	Asp356, Met363, Arg594	Leu283, Gly549, Ala555, Trp481 (2), Met519
	Acarbose ^a	-6.1	2	3	Ala555, Asp404	Arg608, His584, His717
HMGR (PDB: 1HW9)	Diosgenin	-7.9	1	4	Val772	Leu858, Ala754 (3)
	Simvastatin ^a	-5.2	2	4	Ser745, Lys735	Ala754 (3)

^a Standard, **NHBA**: Number of H-bond acceptors, **HBR**: H-bond residues.

indicating more stable surface interactions. Hydrogen bond analysis revealed the formation of one hydrogen bond in both complexes, underscoring a common interaction feature. Molecular Mechanics Poisson-Boltzmann Surface Area (MMPBSA) calculations provided insights into the relative binding energies of the complexes. The PNLIP-diosgenin and PNLIP-orlistat complexes had total binding energies of -79.03 ± 12.18 kJ/mol and -87.44 ± 7.41 kJ/mol, respectively (Table 3). Energy decomposition analysis identified key residues contributing to binding stability. In the PNLIP-diosgenin complex, residues Thr115, Cys181, Gly214, Gly216, Val210, and Gln116 showed the highest energy contributions, whereas in the PNLIP-orlistat complex, Gly216, Val210, Gly214, Thr115, Cys181, and Ile78 were most significant. Some residues, however, were identified as being less favorable for the simulation in both complexes (Fig. 2a–i).

4.5.2. α -glucosidase (GAA) complexed with Momordicoside-I and acarbose

The RMSD for the Momordicoside I-GAA complex and backbone exhibited stable complex formation after an equilibration period of ~ 20 ns at RMSD of ~ 2 Å and 2.5 Å, respectively. The RMSD of both the complex and backbone were stable with a difference of ~ 0.5 Å. In both the complex, RMSF analysis displayed fluctuation in the range of ~ 1 to ~ 7.0 Å. In Momordicoside I-GAA complex, the residues ranging Leu783-Pro793 possessed the higher fluctuation, in which residue Pro790 had the highest RMSF value of 7.2 Å. Additionally, residues leu117-Gln121 of both the complexes possessed fluctuation up to 6.3 Å. In both the complexes, residues involving in ligand binding i.e. Asp356, Met363, Arg594, Leu283, Gly549, Ala555, Trp481, Met519, Ala555, Asp404, Arg608, His584, His717 possessed the least fluctuation (~ 1.5 Å). The radius of gyration (Rg) displays minor fluctuations (steady increase from 28.5 to 28.8 Å) for the Momordicoside I - GAA complex; indicates an opening of binding pocket throughout the simulation period and which ligand gets buried into the binding pocket. However, the Rg was unstable for acarbose-GAA complex. SASA area displayed no fluctuations for both the complexes (steady between ~ 325 nm² to 340 nm²). Finally, number of hydrogen bonds formed were analyzed, in Momordicoside I - GAA complex, 6 hydrogen bonds were formed and 3 were consistent. Likewise, in acarbose - GAA complex 7 hydrogen bonds were formed and 5 were consistent. MMPBSA analysis for Momordicoside I - GAA and acarbose - GAA complex displayed the total relative binding energy of -81.85 ± 15.64 and -722.01 ± 31.2 kJ/mol, respectively (Table 3). The analysis of total energy decomposition showed that in the complex of Momordicoside I and GAA, certain energy components were identified, residues Phe525, Trp481, Leu283, Gly483 possessed the highest energy contribution of -9.49 , -4.55 , -2.74 , -2.14 kJ/mol respectively and Arg281, Asp282 were majorly against the simulation. Likewise, in acarbose - GAA complex Glu721, Glu856, Asp399, Glu748, Asp645, Asp404, Asp406, Glu145 possessed highest energy contribution of -17.90 , -16.56 , -14.29 , -12.54 , -11.60 , -10.52 , -10.01 kJ/mol respectively and Arg331, Arg203, Lys589 were majorly against the simulation (Fig. 3a–i).

4.6. HMG-CoA reductase (HMGR) complexed with diosgenin and simvastatin

The study conducted a detailed analysis of the molecular dynamics of two complexes: the diosgenin-HMGR complex and the simvastatin-HMGR complex which exhibited stable complex formation after an equilibration period of ~ 40 ns at RMSD of ~ 4 Å and 4.5 Å, respectively. Similarly, simvastatin-HMGR complex and backbone exhibited stable complex formation after an equilibration

Table 3

Total relative BE of ligands with prioritized targets.

Energies (kJ/mol)	PNLIP		α -glucosidase		HMGR	
	Diosgenin	Orlistat*	Momordicoside-I	Acarbose*	Diosgenin	Simvastatin*
Δ VDWAALS	-96.47 ± 16.30	-124.3 ± 8.73	-120.3 ± 16.1	-213.5 ± 17.63	-86.73 ± 10.41	-132.98 ± 13.43
Δ EEL	-3.57 ± 4.726	-1.06 ± 9.05	-101.1 ± 19.5	-963.5 ± 36.1	-8.08 ± 9.04	-19.0 ± 11.006
Δ EPB	3.55 ± 13.60	55.86 ± 12.84	155.52 ± 20.63	480.09 ± 22.2	93.46 ± 9.94	95.805 ± 11.061
Δ SASA	-12.53 ± 1.96	-17.85 ± 1.62	-15.83 ± 1.42	-24.99 ± 0.76	-11.14 ± 1.18	-14.86 ± 0.96
Δ TOTAL	-79.03 ± 12.18	-87.44 ± 7.41	-81.85 ± 15.64	-722.01 ± 31.2	-12.48 ± 2.99	-71.05 ± 9.79

The data is displayed as an average with SEM (n = 50); *Standard, Δ VDWAALS: Van Der Waals molecular mechanics energy; Δ EEL: denotes the change in electrostatic molecular mechanics energy; Δ EPB: Polar contribution to the salvation energy; Δ GTOTAL: Total relative binding energy.

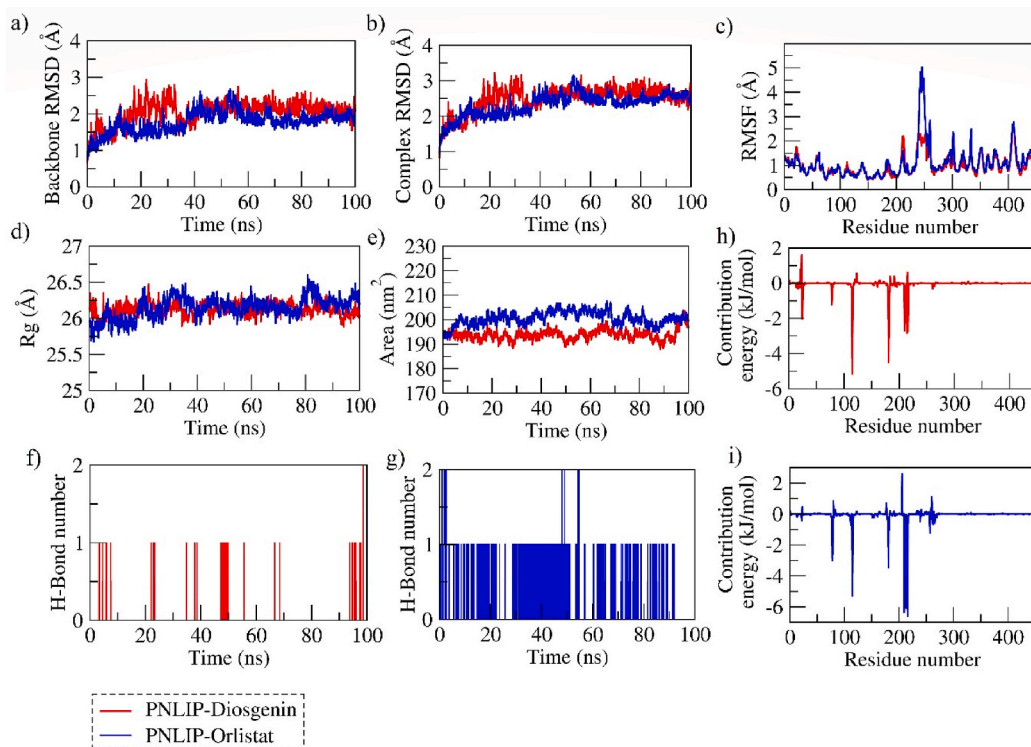


Fig. 2. (a–i). Comparative Analysis of Diosgenin (Red) and Orlistat (Blue) in Interaction with PNLIP. (a) RMSD of the backbone structures; (b) RMSD calculations for the entire complex; (c) RMSF of $C\alpha$ atoms; (d) Assessment of the Radius of Gyration; (e) Evaluation of SASA; (f) and (g) Quantification of hydrogen bonds formed between the compounds and PNLIP during the simulation; and (h) and (i) Analysis of the contribution of each residue to the energy in the formation of a stable complex.

period of ~ 40 ns at RMSD of ~ 3 Å and 3.5 Å, respectively. In both the complex, the N-terminal residues displayed RMS fluctuation of ~ 2.5 Å to ~ 15 Å and the residues involving in ligand binding i.e. Val772, Leu858, Ala754, Ser745, Lys735 possessed the least fluctuation (< 2 Å). The radius of gyration (Rg) displays minor fluctuations (steady at ~ 26 to 28 Å) for the diosgenin - HMGCR complex. However, the Rg was unstable for the simvastatin-HMGCR complex; in which a fluctuation ranged from 28 to 25 Å. The HMGCR-simvastatin complex exhibited fluctuations in SASA from approximately 210 nm²– 205 nm². In contrast, the HMGCR-diosgenin complex showed remarkable stability in SASA, consistently around 215 nm². Finally, number of hydrogen bonds formed were analyzed, in diosgenin - HMGCR complex, 5 hydrogen bonds were formed and 3 were consistent. Likewise, in simvastatin - HMGCR complex 5 hydrogen bonds were formed and 2 were consistent. MMPBSA analysis was performed to evaluate the relative binding energies. The HMGCR-diosgenin complex exhibited a total relative binding energy of -12.48 ± 2.99 kJ/mol. For the HMGCR-simvastatin complex, the binding energy was significantly higher at -71.05 ± 9.79 kJ/mol (Table 3). Energy decomposition analysis further revealed that in the HMGCR-diosgenin complex, residues 693, 702, and 748 showed the highest energy contributions (-6.06 , -5.93 , and -2.43 kJ/mol, respectively). In contrast, the HMGCR-simvastatin complex had its highest contributions from residues Ile762, Thr758, Asn771, Ala768, and Val772, with energy contributions of -7.54 , -5.84 , -3.53 , -3.47 , and -2.92 kJ/mol, respectively (Fig. 4a–i).

4.6.1. PCA of the ligand-protein complex to evaluate the collective motion

To get in-depth understanding of the dynamics exhibited by different complexes, further analysis was done on the resulting trajectory (Fig. 5a–i). PCA aids in comprehending how different conformations evolve throughout simulation. The PNLIP-diosgenin and GAA-Momordicoside I complexes demonstrated cluster evolutions within the conformational ranges of -4 to 3 and -5 to 3 , respectively. This is in contrast to the wider ranges observed in the Diosgenin-HMGCR (-24 to 10) and Simvastatin-HMGCR (-15 to 13) complexes. The study further indicated that the PNLIP-diosgenin complex exhibited a more constrained range of conformational diversity, spanning from -3 to 3 . In comparison, the GAA-acarbose complex displayed a range from -7 to 5 , with eigenvalues of 2 and 6 , respectively. The eigenvalues for the GAA-Momordicoside I and GAA-acarbose complexes were determined to be 7 and 4.5 , respectively. Notably, the Diosgenin and Simvastatin complexes with HMGCR had significantly higher eigenvalues of 65 and 30 , respectively. This suggests that Diosgenin is associated with a greater degree of structural diversity and notable changes in the secondary structure of HMGCR.

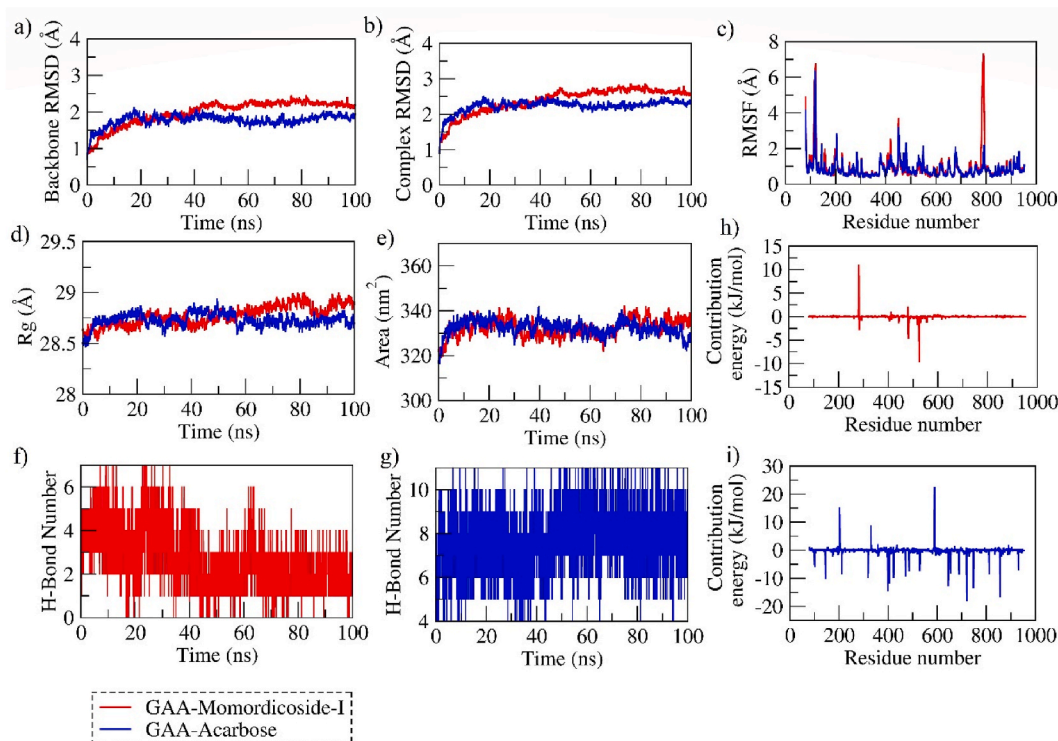


Fig. 3. (a–i): Comparative Analysis of Diosgenin (Red) and Orlistat (Blue) in Interaction with PNLIP. (a) RMSD of the backbone structures; (b) RMSD calculations for the entire complex; (c) RMSF of $C\alpha$ atoms; (d) Assessment of the Radius of Gyration; (e) Evaluation of SASA; (f) and (g) Quantification of hydrogen bonds formed between the compounds and PNLIP during the simulation; and (h) and (i) Analysis of the contribution of each residue to the energy in the formation of a stable complex.

5. Discussion

In this study, the therapeutic efficacy of *Nigella sativa* (NS), *Momordica charantia* (MC), and *Anethum graveolens* (AG) against metabolic syndrome (MetS) targets was examined using both *in vitro* and computational methodologies. A polyherbal formulation was prepared in various NS:MC:AG ratios based on a three-factor, 2-level factorial design, resulting in eight different combinations tested against pancreatic lipase, α -glucosidase, and HMGCR.

Upon evaluating α -glucosidase inhibitory activity, it was observed that acarbose outperformed the sixth formulation (215:50:35 ratio of NS:MC:AG with an IC_{50} of 74.26 g/mL). However, two other formulations also displayed potent inhibitory activities with respective IC_{50} values of 70.44 and 89.74 μ g/mL. The *in-silico* analysis suggested that Momordicoside I (derived from MC) exhibited a higher binding affinity to GAA than acarbose, presenting a potential area for further exploration and understanding. For pancreatic lipase inhibition, the sixth formulation (215:50:35 of NS:MC:AG) showed promising inhibitory activity with an IC_{50} of 74.26 μ g/mL, albeit less potent than orlistat. The computational findings revealed that Diosgenin (from MC) demonstrated a stronger affinity towards PNLIP compared to orlistat, again underscoring a need for deeper examination into this discrepancy. Regarding the inhibition of HMGCR, although Diosgenin manifested a higher affinity towards HMGCR in comparison to simvastatin, *in vitro* assessments indicated that only the eighth formulation exerted some degree of inhibition, suggesting that the individual compounds in the MC might play a significant role in this observed activity [35–43].

Current investigation found that Momordicoside I (from MC) had a higher binding affinity (-8.8 kcal/mol) with GAA than acarbose (-6.1 kcal/mol), indicating that it might be more effective. Hence, the cause for this unexpected result has to be explored further. One explanation could be that the pure medication has a stronger or more powerful inhibitory action than the crude extract. As a result, further research into the effects of Momordicoside I on GAA is required through experimental study. The cucurbitane-type triterpenoids found in bitter melon (MC) have garnered a lot of interest lately owing to the wide range of biological activities they are involved in. More than 240 cucurbitane-type triterpenoids, as well as their glycosides, have been identified and purified from diverse bitter melon plant sections. These chemicals have several biological effects, such as hypoglycemia, anti-obesity, anti-cancer, anti-inflammatory, antioxidant, and anti-inflammatory [44]. In a previous study, momordicoside I, cucurbitane-type triterpene showed α -glucosidase inhibition about 35.1 % at 1.33 mM concentration [44]. While in another study, momordicoside I IC_{50} against α -glucosidase was found to be > 200 μ M and other momordicosides range was from 10 to 200 μ M [45]; indicates enriched fraction could be more potent than individual compound effect. This current study in *silico* investigation revealed inhibition of α -glucosidase via interaction of momordicoside I with Asp356, Met363, Arg594, Leu283, Gly549, Ala555, Trp481, Met519 residues. The molecular

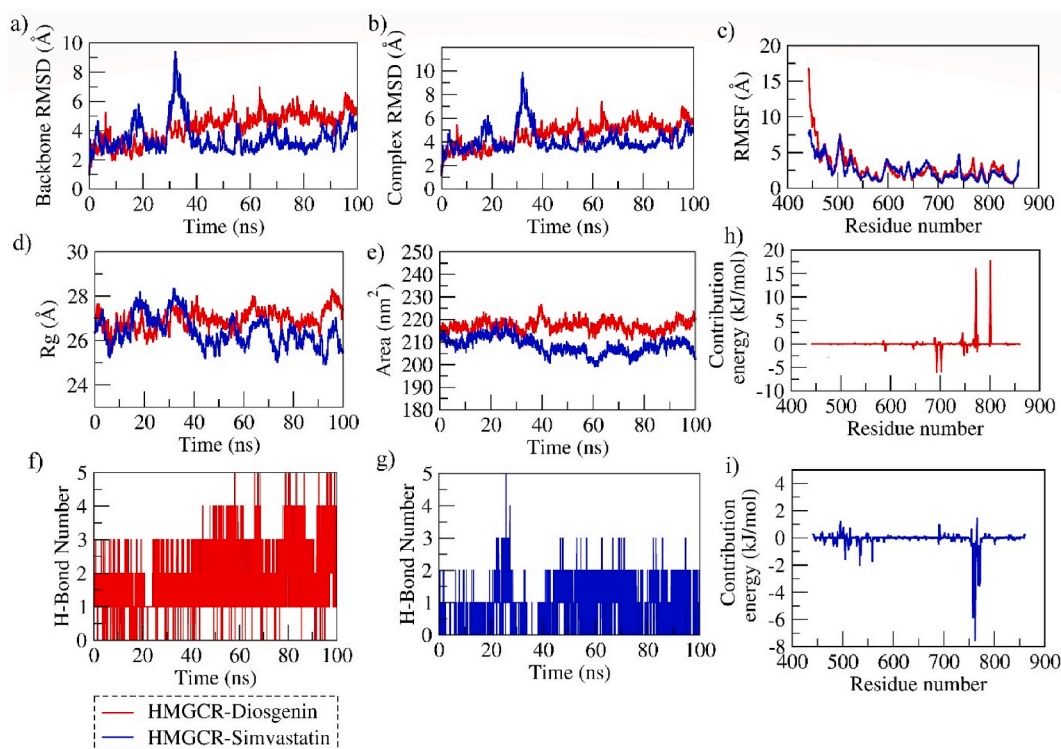


Fig. 4. (a–i). Analysis of Structural Integrity involving Diosgenin (red) and Simvastatin (blue) with PNLIP. (a) Measurement of the backbone RMSD; (b) backbone RMSD; (b) complex RMSD; (c) $C\alpha$ RMSF (d); Radius of gyration; (e) Solvent Assessable Surface Area; (f) and (g) Quantification of the number of hydrogen bonds formed between each compound and HMG-CoA Reductase (HMGCR) throughout the simulation process; and (h) and (i) Each residual contribution energy in stable complex formation.

dynamics also revealed higher stability of momordicoside I with α -glucosidase throughout 100ns MD simulation. While, MMPBSA analysis revealed momordicoside I – GAA complex to display the total relative binding energy of -81.85 ± 15.64 and Phe525, Trp481, Leu283, Gly483 of GAA to possess highest energy contribution of -9.49 , -4.55 , -2.74 , -2.14 kJ/mol with Momordicoside I to form stable complex.

When it comes to the search for promising anti-obesity medicines, the mechanism of pancreatic lipase inhibition has received the greatest attention and research [46]. Pancreatic lipase is secreted by the acinar cells of the pancreas, is an essential enzyme of pancreatic juice that is responsible for the breakdown of dietary lipids in the small intestine. The lipolytic action of pancreatic lipase is facilitated by the pancreatic protein colipase, which functions as a cofactor [43]. In this study, NS:MC:AG at ratio 215:50:35 (formulation No. 6) showed strong inhibitory activity against Pancreatic lipase with IC_{50} of 74.26 μ g/mL, whereas, orlistat IC_{50} was found to be 57.01 μ g/mL; suggesting that it was 0.23 times less potent than orlistat. Along with these, NS:MC:AG at ratio 215:80:25 (formulation No. 7) and ratio 215:80:35 (formulation No. 8) were second and third lead formulations for pancreatic lipase inhibition with IC_{50} of 82.34 and 91.65, respectively. Through *in-silico* molecular docking, we found that diosgenin (from MC) had a higher binding affinity (-11.0 kcal/mol) with PNLIP than orlistat (-7.1 kcal/mol), indicating that it might be more effective. Ile209, Ile78, Pro180, Trp114, Phe215 were the common interacting residues between orlistat and diosgenin. Hence, from experimental and computational study, the cause for this unexpected result has to be explored further. One explanation could be that the pure medication has a stronger or more powerful inhibitory action than the crude extract. As a result, further research into the effects of diosgenin on PNLIP is required through experimental study. The molecular dynamics also revealed higher stability of diosgenin with PNLIP throughout 100ns MD simulation compared to orlistat. While, MMPBSA analysis revealed diosgenin-PNLIP complex to display the total relative binding energy of -79.03 and Thr115, Cys181, Gly214, Gly216, Val210, Gln116 of PNLIP to possess highest energy contribution of 5.17, -4.50 , -2.85 , -2.75 , -2.71 , -2.18 kJ/mol with diosgenin to form stable complex. On the other hand, diosgenin was also found to score the highest binding affinity (-7.9 kcal/mol) with HMGCR compared to simvastatin (-5.2). However, *in vitro* investigation revealed that there is no concentration-dependent inhibition of HMGCR by all the formulations but only formulation number 8 (NS:MC:AG at ratio 215:80:35) showed inhibition at some extent with IC_{50} of 129.03 μ g/mL, whereas, simvastatin IC_{50} was found to be 52.62 μ g/indicating that it was 0.59 times less potent than the simvastatin. This effect could be only due the presence of compounds like momordicosides and diosgenin in MC. Diosgenin is a steroid saponin that is present in a wide range of plant species and is thought to possess a number of intriguing bioactive qualities, including hypoglycaemic, hypolipidemic, antioxidant, anti-inflammatory activities [47]. It is well reported that diosgenin could treat diabetes by increasing adipocyte differentiation and reducing adipose tissue inflammation. Thus, diosgenin may alleviate obesity-related glucose metabolic problem [48]. Diosgenin

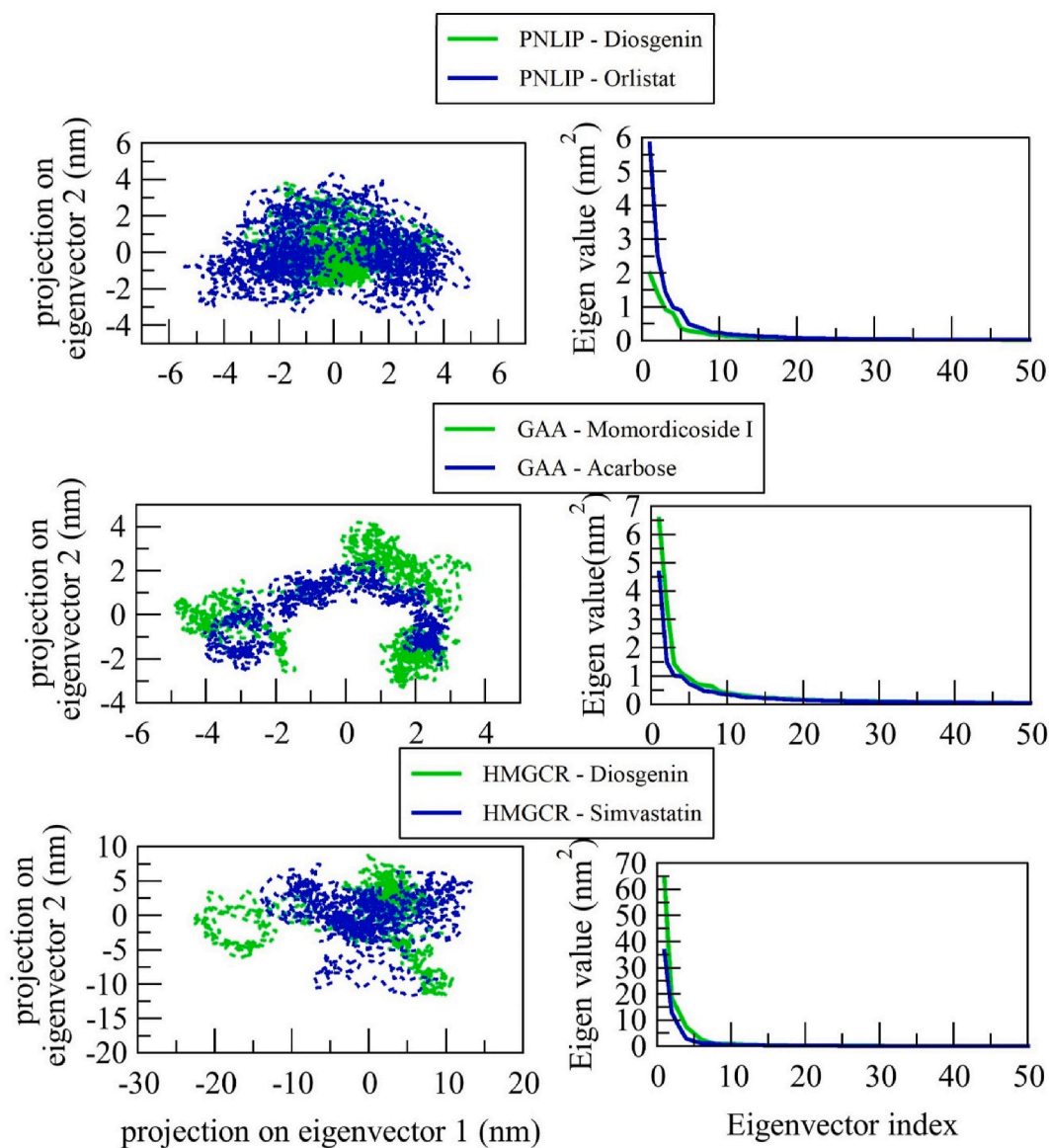


Fig. 5. (a–i): Ligand-protein complexes are subject to principal component analysis. The collective movements of phytocompounds and standard compounds with PNLIP, GAA, and HMGCR utilizing projections of MD trajectories on two eigenvectors corresponding to the first two main components PC1 and PC2. The first 50 eigenvectors were displayed v/s eigenvalues.

reduced plasma and hepatic triglycerides in obese diabetic mice, which may help treat diabetes-related hepatic dyslipidemias [49]. In diosgenin-treated diabetic rats, hyperglycemia, hypercholesterolemia, and hypertriglyceridemia was decreased and PPARs impacted diosgenin's adipogenic action [50]. This steroid reduces intestinal cholesterol absorption and suppresses MiR-19b-induced down-regulation of ATP-binding cassette transporter A1 in macrophages, which contributes to its antiatherogenic actions [51]. Hence, the utilizing momordicosides, diosgenin and/or plant containing them like MC could be beneficial for the management of MetS.

In essence, the intriguing findings of this study shed light on the possible therapeutic potentials of NS, MC, and AG in managing MetS, with particular compounds like Momordicoside I and Diosgenin warranting further investigation. The observed discrepancies between the *in vitro* and *in silico* analyses also highlight the complexity of these bioactive compounds in their interactions with metabolic enzymes, necessitating additional research to unravel their full therapeutic potential and mechanisms of action in MetS treatment.

6. Conclusion

In the current study, we used a poly herbal blend of a mixture of NS, MC, and AG to evaluate its effectiveness towards the MetS

employing *in vitro* enzyme inhibitory activities as well as their mode of inhibition was studied via different molecular modeling methods which includes molecular mechanics and quantum mechanics. This allowed us to determine whether or not the formulation was effective against MetS. In addition, the conclusions depended on the binding affinity and effectiveness of the molecule to influence the intrinsic function, and both dry-lab and wet-lab research. Based to the findings, NS:MC:AG in the following ratios (1) 215:50:35, (2) 215:80:25, and (3) 215:80:35 has the potential to be an efficient treatment for hyperglycemic spikes, obesity, and other comorbidities associated with MetS via inhibiting pancreatic lipase, α -glucosidase, and HMGR. Further, diosgenin and Momordicoside I were the lead hit molecules and are already well established by the numerous researchers and can be utilized them against MetS in the future. In addition to this, further research has to be done to analyze enzyme kinetics, gene expression investigations, and *in vivo* validation and these are the future prospects of the present findings.

Availability of data and materials

All data and material are included within the article.

CRedit authorship contribution statement

Rajashekar S. Chavan: Writing – review & editing, Writing – original draft, Methodology, Investigation, Data curation, Conceptualization. **Nayeem A. Khatib:** Supervision, Methodology, Investigation. **Hariprasad M.G:** Writing – review & editing, Writing – original draft, Methodology, Conceptualization. **Vishal S. Patil:** Methodology, Formal analysis, Data curation. **Moqbel Ali Moqbel Redhwan:** Writing – review & editing, Writing – original draft, Methodology.

Declaration of competing interest

The authors declare that they have no known competing financial interests or personal relationships that could have appeared to influence the work reported in this paper.

Acknowledgments

The authors are thankful to the Principal KLE College of Pharmacy, Belagavi, KAHER, Belagavi for providing the necessary facilities and infrastructure to conduct the research work.

References

- [1] B.L. Graf, I. Raskin, W.T. Cefalu, D.M. Ribnick, Plant-derived therapeutics for the treatment of metabolic syndrome, *Curr. Opin. Invest. Drugs* 11 (10) (2010) 1107 (London, England: 2000).
- [2] Y. Rochlani, N.V. Pothineni, S. Kovelamudi, J.L. Mehta, Metabolic syndrome: pathophysiology, management, and modulation by natural compounds, *Ther Adv Cardiovasc Dis* 11 (8) (2017) 215–225.
- [3] Y. Matsuzawa, T. Funahashi, T. Nakamura, The concept of metabolic syndrome: contribution of visceral fat accumulation and its molecular mechanism, *J. Atherosclerosis Thromb.* 18 (8) (2011) 629–639.
- [4] T. Hiyoshi, M. Fujiwara, Z. Yao, Postprandial hyperglycemia and postprandial hypertriglyceridemia in type 2 diabetes, *Journal of Biomedical Research* 33 (1) (2017) 1–16.
- [5] C.A. Meza, J.D. La Favor, D.H. Kim, R.C. Hickner, Endothelial dysfunction: is there a hyperglycemia-induced imbalance of NOX and NOS? *Int. J. Mol. Sci.* 20 (15) (2019) 3775.
- [6] G. Zhu, Q. Fang, F. Zhu, D. Huang, C. Yang, Structure and function of pancreatic lipase-related protein 2 and its relationship with pathological states, *Front. Genet.* 12 (2021) 693538.
- [7] U. Panwar, S.K. Singh, Identification of novel pancreatic lipase inhibitors using *in silico* studies. *Endocrine, metabolic & immune disorders-drug targets (formerly current drug targets-immune, endocrine & metabolic disorders)* 19 (4) (2019) 449–457.
- [8] P. Khanal, P.S. Dwivedi, V.S. Patil, A. Shetty, A. Aga, A. Javaid, V.V. Bhandare, Barosmin against postprandial hyperglycemia: outputs from computational prediction to functional responses *in vitro*, *J. Biomol. Struct. Dyn.* (2023) 1–7.
- [9] P. Khanal, B.M. Patil, Gene set enrichment analysis of alpha-glucosidase inhibitors from *Ficus benghalensis*, *Asian Pac. J. Trop. Biomed.* 9 (6) (2019) 263–270.
- [10] S. Seshadri, N. Rapaka, B. Prajapati, D. Mandaliya, S. Patel, C.S. Muggalla, et al., Statins exacerbate glucose intolerance and hyperglycemia in a high sucrose fed rodent model, *Sci. Rep.* 9 (1) (2019) 1–9, <https://doi.org/10.1038/s41598-019-45369-8>.
- [11] M. Igel, T. Sudhop, K. von Bergmann, Pharmacology of 3-hydroxy-3-methylglutaryl-coenzyme A reductase inhibitors (statins), including rosuvastatin and pitavastatin, *J. Clin. Pharmacol.* 42 (8) (2002) 835–845, <https://doi.org/10.1177/009127002401102731>.
- [12] P.M. Ridker, A. Pradhan, J.G. MacFadyen, P. Libby, R.J. Glynn, Cardiovascular benefits and diabetes risks of statin therapy in primary prevention: an analysis from the JUPITER trial, *Lancet* 380 (9841) (2012) 565–571, [https://doi.org/10.1016/S0140-6736\(12\)61190-8](https://doi.org/10.1016/S0140-6736(12)61190-8).
- [13] N. Sattar, D. Preiss, H.M. Murray, P. Welsh, B.M. Buckley, A.J. de Craen, et al., Statins and risk of incident diabetes: a collaborative meta-analysis of randomised statin trials, *Lancet* 375 (9716) (2010) 735–742.
- [14] T.T. Nyakudya, T. Tshabalala, R. Dangarembizi, K.H. Erlwanger, A.R. Ndhlala, The potential therapeutic value of medicinal plants in the management of metabolic disorders, *Molecules* 25 (11) (2020) 2669.
- [15] M. Ahmed, N. Kumari, Z. Mirgani, A. Saeed, A. Ramadan, M.H. Ahmed, A.O. Almobarak, Metabolic syndrome; Definition, Pathogenesis, Elements, and the Effects of medicinal plants on its elements, *J. Diabetes Metab. Disord.* 21 (1) (2022) 1011–1022.
- [16] A. Balekundri, A. Shahapuri, M. Patil, Poly-herbal tablet formulation by design expert tool and *in vitro* anti-lipase activity, *Future Journal of Pharmaceutical Sciences* 6 (1) (2020) 1, 1.
- [17] A. Jain, S.K. Jain, Formulation and optimization of temozolomide nanoparticles by 3 factor 2 level factorial design, *Biomatter* 3 (2) (2013) e25102.
- [18] V.P. Gaonkar, V.S. Mannur, V.S. Mastholimath, K.K. Hullatti, Development and evaluation of herbal supplement: a quality by design approach, *Indian J. Pharmaceut. Sci.* 82 (4) (2020).
- [19] R.B. Shete, V.J. Muniswamy, A.P. Pandit, K.R. Khandelwal, Formulation of eco-friendly medicated chewing gum to prevent motion sickness, *AAPS PharmSciTech* 16 (5) (2015) 1041–1050.

- [20] V.L. Singleton, R. Orthofer, R.M. Lamuela-Raventos, Analysis of total phenols and other oxidation substrates and antioxidants by means of Folin-Ciocalteu reagent, *Methods Enzymol.* 299 (1999) 152–179.
- [21] J. Delcour, D.J. Varebeke, Anew colorimetric assay for flavonoids in pilsner beers, *J. Institute. Brewing* 91 (1985) 37–40.
- [22] H.P.S. Makkar, Effect and fate of tannins in ruminant animals, adaptation to tannins and strategies to overcome detrimental effect of feeding tannin-rich feeds, *Small Rumin. Res.* 49 (2003) 241–256.
- [23] M.S. Blois, Antioxidant determinations by the use of a stable free radical, *Nature* 181 (1958) 1199–1200, <https://doi.org/10.1038/1811199a0>.
- [24] Y. Bustanji, A. Issa, M. Mohammad, M. Hudaib, K. Tawah, H. Alkhatib, I. Almasri, B. Al-Khalidi, Inhibition of hormone-sensitive lipase and pancreatic lipase by *Rosmarinus officinalis* extract and selected phenolic constituents, *J. Med. Plants Res.* 4 (2010) 2235–2242.
- [25] C.-D. Zheng, Y.-Q. Duan, J.-M. Gao, Z.-G. Ruan, Screening for anti-lipase properties of 37 traditional Chinese medicinal herbs, *J. Chin. Med. Assoc.* 73 (2010) 319–324.
- [26] P. Khanal, B. Patil, Gene set enrichment analysis of alpha-glucosidase inhibitors from *Ficus benghalensis*, *Asian Pac. J. Trop. Biomed.* 9 (6) (2019) 263–270.
- [27] S. Salvamani, B. Gunasekaran, M.Y. Shukor, N.A. Shaharuddin, M.K. Sabullah, S.A. Ahmad, Anti-HMG-CoA reductase, antioxidant, and anti-inflammatory activities of *Amaranthus viridis* leaf extract as a potential treatment for hypercholesterolemia, *Evid. base Compl. Alternative Med.* (2016) 10.
- [28] M.P. Egloff, F. Marguet, G. Buono, R. Verger, C. Cambillau, H. van Tilbeurgh, The 2.46. ANG. resolution structure of the pancreatic lipase-colipase complex inhibited by a C11 alkyl phosphonate, *Biochemistry* 34 (9) (1995 Mar 1) 2751–2762.
- [29] V. Roig-Zamboni, B. Cobucci-Ponzano, R. Iacono, M.C. Ferrara, S. Germany, Y. Bourne, G. Parenti, M. Moracci, G. Sulzenbacher, Structure of human lysosomal acid α -glucosidase—a guide for the treatment of Pompe disease, *Nat. Commun.* 8 (1) (2017 Oct 24) 1111.
- [30] E.S. Istvan, J. Deisenhofer, Structural mechanism for statin inhibition of HMG-CoA reductase, *Science* 292 (5519) (2001 May 11) 1160–1164.
- [31] A. Samdani, U. Vetrivel, POAP: a GNU parallel based multithreaded pipeline of open babel and AutoDock suite for boosted high throughput virtual screening, *Comput. Biol. Chem.* 74 (2018 Jun 1) 39–48.
- [32] D. Van Der Spoel, E. Lindahl, B. Hess, G. Groenhof, A.E. Mark, H.J. Berendsen, GROMACS: fast, flexible, and free, *J. Comput. Chem.* 26 (16) (2005) 1701–1718.
- [33] R. Kumari, R. Kumar, A. Lynn, g_mmpbsa—a GROMACS tool for high-throughput MM-PBSA calculations, *J. Chem. Inf. Model.* 54 (7) (2014) 1951–1962.
- [34] K. Bhattacharya, P. Khanal, V.S. Patil, P.S. Dwivedi, N.R. Chanu, R.K. Chaudhary, S. Deka, A. Chakraborty, Computational pharmacology profiling of borapetoside C against melanoma, *J. Biomol. Struct. Dyn.* (2023 May 11) 1–6.
- [35] B. Hess, Similarities between principal components of protein dynamics and random diffusion. *Physical Review, E, Statistical Physics, Plasmas, Fluids, and Related Interdisciplinary Topics* 62 (6 Pt B) (2000) 8438–8448.
- [36] S.R. Shivanagoudra, W.H. Perera, J.L. Perez, G. Athrey, Y. Sun, C.S. Wu, G.K. Jayaprakasha, B.S. Patil, In vitro and in silico elucidation of antidiabetic and anti-inflammatory activities of bioactive compounds from *Momordica charantia* L, *Bioorg. Med. Chem.* 27 (14) (2019 Jul 15) 3097–3109.
- [37] J. Yue, J. Xu, J. Cao, X. Zhang, Y. Zhao, Cucurbitane triterpenoids from *Momordica charantia* L. and their inhibitory activity against α -glucosidase, α -amylase and protein tyrosine phosphatase 1B (PTP1B), *J. Funct. Foods* 37 (2017) 624–631.
- [38] N.A. Lunagariya, N.K. Patel, S.C. Jagtap, K.K. Bhutani, Inhibitors of pancreatic lipase: state of the art and clinical perspectives, *EXCLI J* 13 (2014 Aug 22) 897–921.
- [39] M. Jesus, A.P. Martins, E. Gallardo, S. Silvestre, Diosgenin: recent highlights on pharmacology and analytical methodology, *Journal of analytical methods in chemistry* (2016), 2016 Oct.
- [40] T. Uemura, S. Hirai, N. Mizoguchi, et al., Diosgenin present in fenugreek improves glucose metabolism by promoting adipocyte differentiation and inhibiting inflammation in adipose tissues, *Mol. Nutr. Food Res.* 54 (11) (2010) 1596–1608.
- [41] T. Uemura, T. Goto, M.-S. Kang, et al., Diosgenin, the main aglycon of fenugreek, inhibits LXR α activity in HepG2 cells and decreases plasma and hepatic triglycerides in obese diabetic mice, *J. Nutr.* 141 (1) (2011) 17–23.
- [42] M.K. Sangeetha, N. Shrishri Mal, K. Atmaja, V.K. Sali, H.R. Vasanthi, PPAR's and Diosgenin a chemico biological insight in NIDDM, *Chem. Biol. Interact.* 206 (2) (2013) 403–410.
- [43] Y.-C. Lv, J. Yang, F. Yao, et al., Diosgenin inhibits atherosclerosis via suppressing the MiR-19b-induced downregulation of ATP-binding cassette transporter A1, *Atherosclerosis* 240 (1) (2015) 80–89.
- [44] S.R. Shivanagoudra, W.H. Perera, J.L. Perez, G. Athrey, Y. Sun, C.S. Wu, G.K. Jayaprakasha, B.S. Patil, In vitro and in silico elucidation of antidiabetic and anti-inflammatory activities of bioactive compounds from *Momordica charantia* L, *Bioorg. Med. Chem.* 27 (14) (2019 Jul 15) 3097–3109.
- [45] J. Yue, J. Xu, J. Cao, X. Zhang, Y. Zhao, Cucurbitane triterpenoids from *Momordica charantia* L. and their inhibitory activity against α -glucosidase, α -amylase and protein tyrosine phosphatase 1B (PTP1B), *J. Funct. Foods* 37 (2017) 624–631.
- [46] N.A. Lunagariya, N.K. Patel, S.C. Jagtap, K.K. Bhutani, Inhibitors of pancreatic lipase: state of the art and clinical perspectives, *EXCLI J* 13 (2014 Aug 22) 897–921.
- [47] M. Jesus, A.P. Martins, E. Gallardo, S. Silvestre, Diosgenin: recent highlights on pharmacology and analytical methodology, *Journal of analytical methods in chemistry* (2016), 2016 Oct.
- [48] T. Uemura, S. Hirai, N. Mizoguchi, et al., Diosgenin present in fenugreek improves glucose metabolism by promoting adipocyte differentiation and inhibiting inflammation in adipose tissues, *Mol. Nutr. Food Res.* 54 (11) (2010) 1596–1608.
- [49] T. Uemura, T. Goto, M.-S. Kang, et al., Diosgenin, the main aglycon of fenugreek, inhibits LXR α activity in HepG2 cells and decreases plasma and hepatic triglycerides in obese diabetic mice, *J. Nutr.* 141 (1) (2011) 17–23.
- [50] M.K. Sangeetha, N. Shrishri Mal, K. Atmaja, V.K. Sali, H.R. Vasanthi, PPAR's and Diosgenin a chemico biological insight in NIDDM, *Chem. Biol. Interact.* 206 (2) (2013) 403–410.
- [51] Y.-C. Lv, J. Yang, F. Yao, et al., Diosgenin inhibits atherosclerosis via suppressing the MiR-19b-induced downregulation of ATP-binding cassette transporter A1, *Atherosclerosis* 240 (1) (2015) 80–89.